

Magnetic properties of 3d, 4d, and 5d transition-metal atomic monolayers in Fe/TM/Fe sandwiches: Systematic first-principles study

Justyn Snarski-Adamski*, Justyna Rychły, Mirosław Werwiński

*Institute of Molecular Physics, Polish Academy of Sciences,
M. Smoluchowskiego 17, 60-179 Poznań, Poland*

Abstract

Previous studies have accurately determined the effect of transition metal point defects on the properties of bcc iron. The magnetic properties of transition metal monolayers on the iron surfaces have been studied equally intensively. In this work, we investigated the magnetic properties of the 3d, 4d, and 5d transition-metal (TM) atomic monolayers in Fe/TM/Fe sandwiches using the full-potential local-orbital (FPLO) scheme of density functional theory. We prepared models of Fe/TM/Fe structures using the supercell method. We selected the total thickness of our system so that the Fe atomic layers furthest from the TM layer exhibit bulk iron-bcc properties. Along the direction perpendicular to the TM layer, we observe oscillations of spin and charge density. For Pt and W we obtained the largest values of perpendicular magnetocrystalline anisotropy and for Lu and Ir the largest values of in-plane magnetocrystalline anisotropy. All TM layers, except Co and Ni, reduce the total spin magnetic moment in the generated models, which is in good agreement with the Slater-Pauling curve. Density of states calculations showed that for Ag, Pd, Ir, and Au monolayers, a distinct van Hove singularity associated with TM/Fe interface can be observed at the Fermi level.

1. Introduction

Over the past decades, the magnetic thin films and layered structures have attracted considerable attention in theoretical and applied physics [1]. These systems exhibit novel physical phenomena such as enhanced magnetic moments, magnetocrystalline anisotropy (MAE), oscillatory interlayer coupling, and spin and charge-density waves [2, 3]. These quantum phenomena related to magnetism and spin-orbit coupling are also the subject of interest in spintronics. An important example of a spintronic device is the spin-transfer torque memory, which uses a spin-polarized tunneling current to switch magnetization [4]. Although there is huge potential in creating mag-

netic multilayer structures, their control is difficult. Moreover, controlling and growing clean and sharp interfaces requires a large amount of labor and knowledge. Previous studies have predicted strong effects of 3d TM monolayers on ferromagnetic moments on metallic overlayers [5, 6] or sandwich bilayers [7]. For the systems considering the sandwiches model with Mn bilayers, oscillations of spin magnetic moments were observed [7]. The magnetic properties of 3d TM on metallic substrates such as Pd(001) and Ag(001) show great similarity to the interactions of 3d magnetic impurities in bulk alloys [8]. For 4d and 5d monolayer on Ag(001) and Au(001) substrates, the magnetism has been explained as real effect of two-dimensional band structure [9]. An exceptionally large perpendicular MAE was found for Ir monolayer capped on Fe(001) surface [10]. There has also been interest in forcing ferromagnetic cou-

*Corresponding author

Email address: justyn.snarski-adamski@ifmpan.poznan.pl
(Justyn Snarski-Adamski)

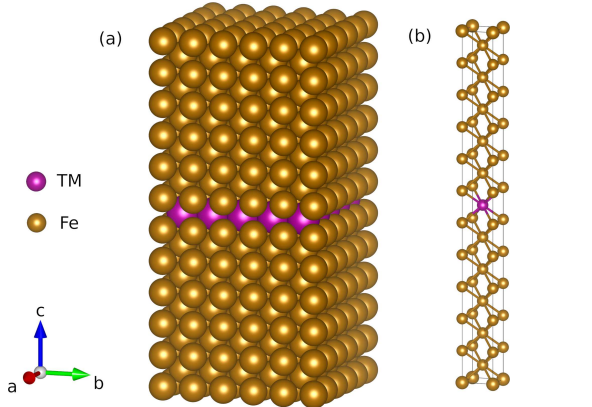


Figure 1: A model of the crystal structure of the Fe/TM/Fe-sandwich system which crystallizes in a tetragonal structure [space group $P4/mmm$ (No. 123), $a = b = 2.83 \text{ \AA}$ and $c = 31.13 \text{ \AA}$]. (a) Model showing the periodic multiplication of the unit cell, which is the subject of our consideration. (b) Unit cell of the Fe/TM/Fe-sandwich system.

pling in rare-earth-metal/Fe sandwiches systems using $3d$ elements, which allow to obtain huge magnetic moments of the order of $10 \mu_B/\text{rare-earth atom}$ [11, 12]. Furthermore, the ferromagnetic coupling in the Fe/TM/Gd sandwich system with $4d$ and $5d$ metal spacers was found to be stronger than that with $3d$ spacers [13]. In this work, we focused on the systems consisting of a Fe-bcc matrix and a transition metal monolayer, see Fig. 1.

2. Computational details

In this paper, the results of computations performed in the framework of density functional theory (DFT) are presented. The models of $3d$, $4d$, and $5d$ transition-metal atomic monolayers in Fe/TM/Fe sandwiches were investigated using the full-potential local-orbital scheme (FPLO18.00-52) [14, 15]. To model the systems, we used the supercell method [16]. The structural parameters of our models are $a = b = 2.83 \text{ \AA}$ and $c = 31.13 \text{ \AA}$. The generalized gradient approximation (GGA) in the Perdew-Burke-Ernzerhof (PBE) form [17] was used. The lattice parameters were set as for bulk Fe-bcc and multiply 11 times in the c direction, whereas the Wyckoff positions were optimized for each considered system using a spin-

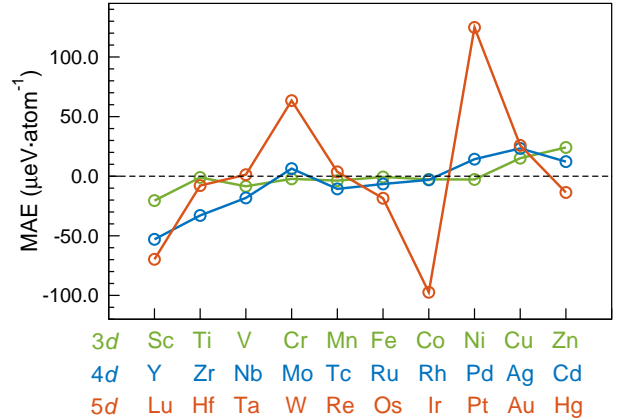


Figure 2: Magnetocrystalline anisotropy energy (MAE) of Fe/TM/Fe-sandwiches for various $3d$, $4d$, and $5d$ transition metal (TM) elements. Calculations were performed with the FPLO18 using the PBE functional and supercell model. Considered unit cell include 21 atoms of Fe and 1 atom of TM.

polarized scalar-relativistic approach, see Fig. 1. The substitution of TM element was intended to create a single dopant monolayer in the center of this structure. Our calculation did not include optimization of lattice parameters. A $12 \times 12 \times 1$ k -mesh was used for geometrical optimization and accuracy of forces was set as $10^{-3} \text{ eV \AA}^{-1}$. An $80 \times 80 \times 10$ k -mesh was found to lead to well converged results of the magnetocrystalline anisotropy energies (MAE). The convergence criterion for the charge density was set as 10^{-6} . MAE was evaluated as a difference between the fully-relativistic total energies calculated for quantization axes [100] and [001]. The applied full-potential approach plays an important role in the correct determination of the values of magnetic moments and MAE [18]. For Fe₂₂, the obtained result of the MAE value determines the accuracy of our calculations, as we would expect zero for such a system. Thus, the accuracy of our calculations is estimated at $1 \mu\text{eV}/\text{atom}$. The VESTA code was used to visualize the crystal structure [19].

3. Results and discussion

Since we considered all $3d$, $4d$, and $5d$ transition metals in Fe/TM/Fe-sandwich models, we obtained a complete

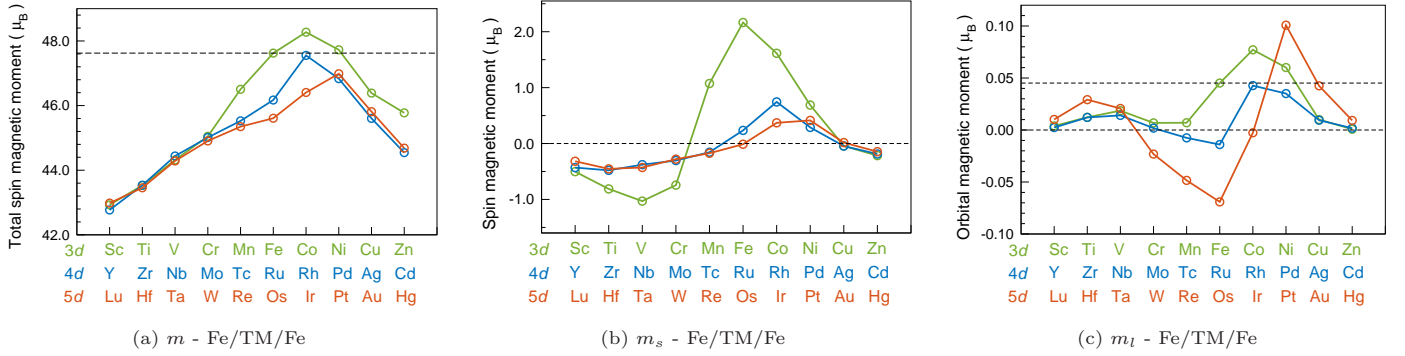


Figure 3: (a) Total spin magnetic moment per formula unit, (b) spin magnetic moment as calculated for spin quantization axis along the distinguished axis [001] (easy axis), (c) orbital magnetic moment as calculated for spin quantization axis along the [001] (easy axis) for various 3d, 4d, and 5d TM elements in the Fe/TM/Fe-sandwiches. Calculations were performed with FPLO18, using the PBE functional and supercell method.

picture of the variations of MAE, total spin magnetic moment, and magnetic moments on TM, see Figs. 3b and 3c. We can see that 5d elements can lead to a more extreme MAE than the 3d and 4d elements due to the stronger spin-orbit coupling. Positive and negative MAE values indicate alignment of magnetic moments perpendicular and in-plane of the TM layer, respectively. For Pt and W we obtained the largest values of perpendicular magnetocrystalline anisotropy and for Lu and Ir the largest values of in-plane magnetocrystalline anisotropy. The largest value of MAE for Pt interlayer is not surprising considering the extremely high MAE values observed for the L1₀ FePt phase [20]. The previous calculations also showed an increase in the value of MAE for systems with W substitution [18, 21].

Almost all TM elements, except Co and Ni, decrease the total spin magnetic moment relative to the Fe atom in the structures under our consideration, see Fig. 3a, which is in good agreement with the Slater-Pauling curve [22]. We also see that almost all TMs, except Co, Ni, and Pt, contribute a lower orbital magnetic moment than Fe, see Fig. 3c. Against this background, Pt stands out again, as it has the highest orbital moment among all the TMs considered. The orbital magnetic moment for bcc Fe calculated in this paper, which is 0.045 μ_B , is underestimated relative to the experimental value of 0.085 μ_B , which suggests that the calculated values of orbital magnetic moment are

about twice underestimated. [23]. Calculations of the spin and orbital magnetic moment on the atomic monolayer of the transition metal show explicit trends with increasing atomic numbers. Analogous trends have been found for point substitutions in bulk-iron, both theoretically [24, 25] and experimentally [26].

Therefore, we conducted a detailed case study for a system with Pt for which we obtained the maximum value of MAE. In Fig. 4a, we have shown the oscillation of charge and spin magnetic moment in Fe/Pt/Fe-sandwich system. For Pt we observe spin magnetic moment of 0.42 μ_B and for three Fe layers nearest to Pt the values are as follows: 2.76, 2.32, and 2.25 μ_B . However, the Fe layers farthest from the Pt layer exhibit bulk Fe-bcc magnetic properties.

We present the calculation of density of states to show what happens near the interface in the Fe/Pt/Fe-sandwich, see Fig. 5. In Fig. 5b we present the total DOS for the Fe/Pt/Fe system with the comparisons in Fig. 5a for Fe₂₂-bcc in the same model as here discussed (Fe/Fe/Fe-sandwich system). The comparison of Fe₂₂ DOS with Fe/Pt/Fe DOS shows great similarity and few differences resulting from about two additional electrons on the Pt 5d shell compared to the Fe 3d shell. The c-g panels show the contributions from the d orbitals the two closest (Fe1, Fe2) and farthest (F10, Fe11) Fe layers in relation to the Pt layer. For the Pt 5d band, one spin channel

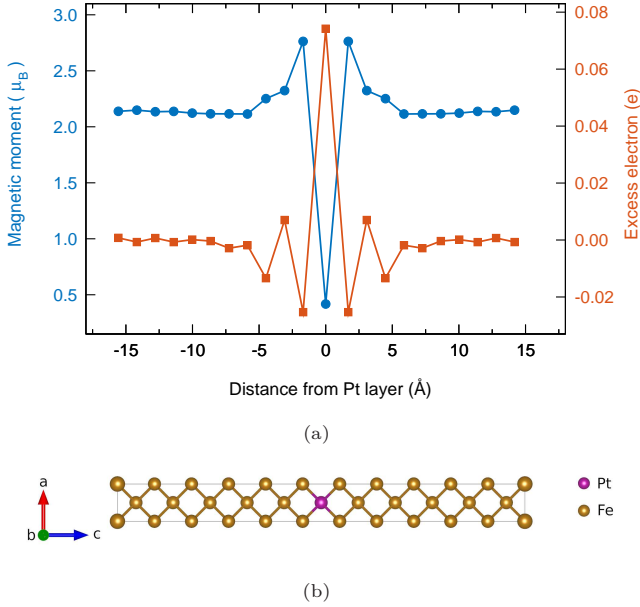


Figure 4: (a) Calculation of spin magnetic moment and charge oscillations in Fe/Pt/Fe-sandwich system. (b) A model of the crystal structure of Fe/TM/Fe-sandwich.

is partially empty and the other is completely filled. The adjacent Fe1 layer shows an increased spin polarization value ($m_s = 2.76 \mu_B$). The DOS for Fe10 and Fe11, farthest from Pt layer, resemble the spectra observed for Fe₂₂. The van Hove singularity on the Fermi level observed for Fe/Pt/Fe-sandwich system comes from the Pt 5d states. This narrow maximum at the Fermi level can have a significant impact on the electrochemical properties of the considered system. Unlike the band-types typical of valence band states, it can be interpreted as a characteristic of an atomic-like state of electrons.

4. Summary and conclusions

We have presented the first-principles results for the Fe/TM/Fe-sandwich system. Almost all TM layers, except Co and Ni layers, reduce the total spin magnetic moment in the considered models, which agrees well with the Slater-Pauling curve. We observe that W and Pt monolayers induce strong perpendicular magnetocrys-

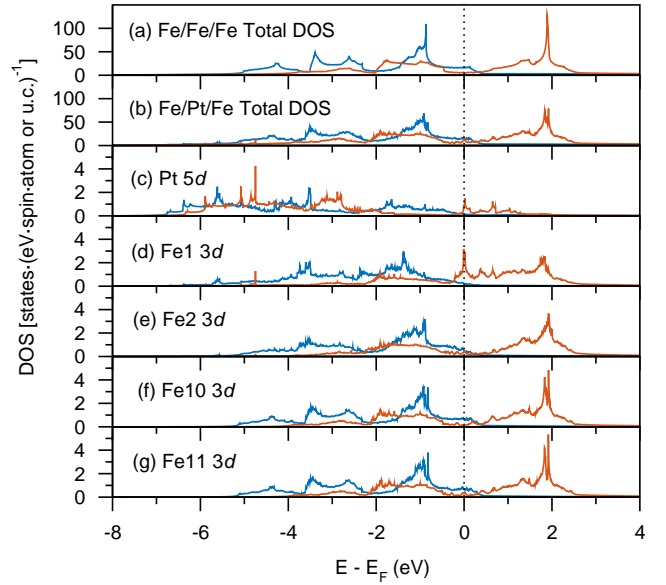


Figure 5: Calculated densities of states (DOS) for the considered Fe/TM/Fe structure. (a) Fe₂₂ total DOS, (b) Fe/Pt/Fe total DOS, (c) Pt 5d DOS, (d, e) Fe1 and Fe2 3d DOS for the two Fe layers closest to the Pt layer, (f, g) Fe10 and Fe11 3d DOS for the two Fe layers furthest from the Pt layer.

talline anisotropy, while Lu and Ir most strongly prefer in-plane anisotropy. Our calculations indicate oscillation of spin magnetic moment and charge. We have also observed the van Hove singularity in the formed Fe/TM interface for TM = Ag, Pd, Pt, Ir, and Au.

Acknowledgements

We acknowledge the financial support of the National Science Center Poland under the decision DEC-2019/35/O/ST5/02980 (PRELUDIUM-BIS 1) and DEC-2018/30/E/ST3/00267 (SONATA-BIS 8). Part of the computations were performed on resources provided by the Poznan Supercomputing and Networking Center (PSNC). We thank Paweł Leśniak and Daniel Depcik for compiling the scientific software and administration of the computing cluster at the Institute of Molecular Physics, Polish Academy of Sciences.

Appendix

Table 1 provides the values shown in Figs. 2, 3a, 3b, and 3c.

References

- [1] T. Thersleff, S. Muto, M. Werwinski, J. Spiegelberg, Y. Kvashnin, B. Hjorvarsson, O. Eriksson, J. Ruzs, K. Leifer, Towards sub-nanometer real-space observation of spin and orbital magnetism at the Fe/MgO interface, *Sci. Rep.* 7 (1) (2017) 44802. doi:10.1038/srep44802.
- [2] R. S. Fishman, Spin-density waves in Fe/Cr trilayers and multilayers, *J. Phys. Condens. Matter* 13 (13) (2001) R235–R269. doi:10.1088/0953-8984/13/13/201.
- [3] C. Turtur, G. Bayreuther, Magnetic moments in ultrathin Cr films on Fe(100), *Phys. Rev. Lett.* 72 (10) (1994) 1557–1560. doi:10.1103/PhysRevLett.72.1557.
- [4] J. C. Slonczewski, Current-driven excitation of magnetic multilayers, *J. Magn. Magn. Mater.* 159 (1) (1996) L1–L7. doi:10.1016/0304-8853(96)00062-5.
- [5] C. L. Fu, A. J. Freeman, T. Oguchi, Prediction of Strongly Enhanced Two-Dimensional Ferromagnetic Moments on Metallic Overlayers, Interfaces, and Superlattices, *Phys. Rev. Lett.* 54 (25) (1985) 2700–2703. doi:10.1103/PhysRevLett.54.2700.
- [6] C. Li, A. J. Freeman, Giant monolayer magnetization of Fe on MgO: A nearly ideal two-dimensional magnetic system, *Phys. Rev. B* 43 (1) (1991) 780–787. doi:10.1103/PhysRevB.43.780.
- [7] S. T. Purcell, M. T. Johnson, N. W. E. McGee, R. Coehoorn, W. Hoving, Two-monolayer oscillations in the antiferromagnetic exchange coupling through Mn in Fe/Mn/Fe sandwich structures, *Phys. Rev. B* 45 (22) (1992) 13064–13067. doi:10.1103/PhysRevB.45.13064.
- [8] S. Blügel, B. Drittler, R. Zeller, P. H. Dederichs, Magnetic properties of 3d transition metal monolayers on metal substrates, *Appl. Phys. A* 49 (6) (1989) 547–562. doi:10.1007/BF00616980.
- [9] S. Blügel, Two-dimensional ferromagnetism of 3d, 4d, and 5d transition metal monolayers on noble metal (001) substrates, *Phys. Rev. Lett.* 68 (6) (1992) 851–854. doi:10.1103/PhysRevLett.68.851.
- [10] D. Odkhui, S. H. Rhim, N. Park, S. C. Hong, Extremely large perpendicular magnetic anisotropy of an Fe(001) surface capped by 5d transition metal monolayers: A density functional study, *Phys. Rev. B* 88 (18) (2013) 184405. doi:10.1103/PhysRevB.88.184405.
- [11] B. Sanyal, C. Antoniak, T. Burkert, B. Krumme, A. Warland, F. Stromberg, C. Praetorius, K. Fauth, H. Wende, O. Eriksson, Forcing Ferromagnetic Coupling Between Rare-Earth-Metal and 3d Ferromagnetic Films, *Phys. Rev. Lett.* 104 (15) (2010) 156402. doi:10.1103/PhysRevLett.104.156402.
- [12] C. Autieri, P. A. Kumar, D. Walecki, S. Webers, M. A. Gubbins, H. Wende, B. Sanyal, Recipe for High Moment Materials with Rare-Earth and 3d Transition Metal Composites, *Sci. Rep.* 6 (1) (2016) 29307. doi:10.1038/srep29307.
- [13] C. Autieri, B. Sanyal, A systematic study of 4d and 5d transition metal mediated exchange coupling between Fe and Gd nanolaminates, *J. Phys. Condens. Matter* 29 (46) (2017) 465802. doi:10.1088/1361-648X/aa8f1e.
- [14] K. Koepnik, H. Eschrig, Full-potential nonorthogonal local-orbital minimum-basis band-structure scheme, *Phys. Rev. B* 59 (3) (1999) 1743–1757. doi:10.1103/PhysRevB.59.1743.
- [15] H. Eschrig, 2. The Essentials of Density Functional Theory and the Full-Potential Local-Orbital Approach, in: W. Hergert, M. Däne, A. Ernst (Eds.), *Computational Materials Science: From Basic Principles to Material Properties*, Lecture Notes in Physics, Springer, Berlin, Heidelberg, 2004, pp. 7–21. doi:10.1007/978-3-540-39915-5_2.
- [16] A. Edström, Magnetocrystalline anisotropy of Laves phase Fe₂Ta_{1-x}W_x from first principles: Effect of 3d-5d hybridization, *Phys. Rev. B* 96 (6) (2017) 064422. doi:10.1103/PhysRevB.96.064422.
- [17] J. P. Perdew, K. Burke, M. Ernzerhof, Generalized Gradient Approximation Made Simple, *Phys. Rev. Lett.* 77 (18) (1996) 3865–3868. doi:10.1103/PhysRevLett.77.3865.
- [18] M. Werwiński, A. Edström, J. Ruzs, D. Hedlund, K. Gunnarsson, P. Svedlindh, J. Cedervall, M. Sahlberg, Magnetocrystalline anisotropy of Fe₅PB₂ and its alloys with Co and 5d elements: A combined first-principles and experimental study, *Phys. Rev. B* 98 (21) (2018) 214431. doi:10.1103/PhysRevB.98.214431.
- [19] K. Momma, F. Izumi, *VESTA* : A three-dimensional visualization system for electronic and structural analysis, *J. Appl. Crystallogr.* 41 (3) (2008) 653–658. doi:10.1107/S0021889808012016.
- [20] R. A. Ristau, K. Barmak, L. H. Lewis, K. R. Coffey, J. K. Howard, On the relationship of high coercivity and L10 ordered phase in CoPt and FePt thin films, *J. Appl. Phys.* 86 (8) (1999) 4527–4533. doi:10.1063/1.371397.
- [21] A. Edström, M. Werwiński, D. Iuşan, J. Ruzs, O. Eriksson, K. P. Skokov, I. A. Radulov, S. Ener, M. D. Kuz'min, J. Hong, M. Fries, D. Y. Karpenkov, O. Gutfleisch, P. Toson, J. Fidler, Magnetic properties of (Fe_{1-x}Co_x)₂B alloys and the effect of doping by 5d elements, *Phys. Rev. B* 92 (17) (2015) 174413.

Table 1: Values of magnetocrystalline anisotropy energy [MAE ($\mu\text{eV}/\text{atom}$)], total spin magnetic moment [m (μ_B u.c. $^{-1}$)], spin magnetic moment [m_s (μ_B u.c. $^{-1}$)] on transition metal (TM), and orbital magnetic moment [m_l (μ_B u.c. $^{-1}$)] on TM for various $3d$, $4d$, and $5d$ TM elements in the Fe/TM/Fe-sandwiches.

$3d$					$4d$					$5d$				
TM	MAE	m	m_s	m_l	TM	MAE	m	m_s	m_l	TM	MAE	m	m_s	m_l
Sc	-20.46	42.93	-0.50	0.0039	Y	-52.96	42.77	-0.43	0.0024	Lu	-69.73	42.98	-0.32	0.0102
Ti	-1.06	43.53	-0.81	0.0123	Zr	-32.93	43.54	-0.48	0.0121	Hf	-7.88	43.46	-0.45	0.0292
V	-8.47	44.32	-1.03	0.0186	Nb	-18.24	44.44	-0.38	0.0141	Ta	1.27	44.29	-0.43	0.0207
Cr	-2.25	45.05	-0.74	0.0068	Mo	6.38	45.01	-0.30	0.0018	W	63.41	44.91	-0.28	-0.0232
Mn	-3.69	46.50	1.07	0.0070	Tc	-10.62	45.53	-0.16	-0.0075	Re	3.65	45.35	-0.17	-0.0484
Fe	-0.63	47.62	2.16	0.0451	Ru	-6.52	46.17	0.23	-0.0140	Os	-18.48	45.61	-0.01	-0.0692
Co	-2.67	48.27	1.61	0.0771	Rh	-3.06	47.55	0.74	0.0427	Ir	-97.39	46.41	0.37	-0.0027
Ni	-2.76	47.73	0.69	0.0601	Pd	14.28	46.83	0.29	0.0351	Pt	124.80	46.99	0.41	0.1008
Cu	15.08	46.39	-0.04	0.0101	Ag	23.30	45.60	-0.05	0.0094	Au	25.82	45.81	0.02	0.0425
Zn	24.08	45.77	-0.22	0.0008	Cd	12.22	44.54	-0.19	0.0017	Hg	-13.64	44.68	-0.15	0.0092

[doi:10.1103/PhysRevB.92.174413](https://doi.org/10.1103/PhysRevB.92.174413).

- [22] A. Williams, V. Moruzzi, A. Malozemoff, K. Terakura, Generalized Slater-Pauling curve for transition-metal magnets, IEEE Trans. Magn. 19 (5) (1983) 1983–1988. [doi:10.1109/TMAG.1983.1062706](https://doi.org/10.1109/TMAG.1983.1062706).
- [23] C. T. Chen, Y. U. Idzerda, H.-J. Lin, N. V. Smith, G. Meigs, E. Chaban, G. H. Ho, E. Pellegrin, F. Sette, Experimental Confirmation of the X-Ray Magnetic Circular Dichroism Sum Rules for Iron and Cobalt, Phys. Rev. Lett. 75 (1) (1995) 152–155. [doi:10.1103/PhysRevLett.75.152](https://doi.org/10.1103/PhysRevLett.75.152).
- [24] H. Akai, Nuclear spin-lattice relaxation of impurities in ferromagnetic iron, Hyperfine Interact. 43 (1) (1988) 253–270. [doi:10.1007/BF02398306](https://doi.org/10.1007/BF02398306).
- [25] P. H. Dederichs, R. Zeller, H. Akai, H. Ebert, Ab-initio calculations of the electronic structure of impurities and alloys of ferromagnetic transition metals, J. Magn. Magn. Mater. 100 (1) (1991) 241–260. [doi:10.1016/0304-8853\(91\)90823-S](https://doi.org/10.1016/0304-8853(91)90823-S).
- [26] R. Wienke, G. Schütz, H. Ebert, Determination of local magnetic moments of 5d impurities in Fe detected via spin-dependent absorption, J. Appl. Phys. 69 (8) (1991) 6147–6149. [doi:10.1063/1.348786](https://doi.org/10.1063/1.348786).